Mutational Analysis Reveals a Role for the C Terminus of the Proteasome Subunit Rpt4p in Spindle Pole Body Duplication in *Saccharomyces cerevisiae*

Heather B. McDonald,*,[1] Astrid Hoes Helfant,*,[2] Erin M. Mahony,* Shaun K. Khosla* and Loretta Goetsch†

**Department of Biology, Colgate University, Hamilton, New York 13346 and †Department of Genome Sciences, University of Washington, Seattle, Washington 98195*

Manuscript received May 29, 2002
Accepted for publication July 24, 2002

ABSTRACT

The ubiquitin/proteasome pathway plays a key role in regulating cell cycle progression. Previously, we reported that a conditional mutation in the *Saccharomyces cerevisiae* gene *RPT4/PCS1*, which encodes one of six ATPases in the proteasome 19S cap complex/regulatory particle (RP), causes failure of spindle pole body (SPB) duplication. To improve our understanding of Rpt4p, we created 58 new mutations, 53 of which convert clustered, charged residues to alanine. Virtually all mutations that affect the N-terminal region, which contains a putative nuclear localization signal and coiled-coil motif, result in a wild-type phenotype. Nine mutations that affect the central ATPase domain and the C-terminal region confer recessive lethality. The two conditional mutations identified, *rpt4-145* and *rpt4-150*, affect the C terminus. After shift to high temperature, these mutations generally cause cells to progress slowly through the first cell cycle and to arrest in the second cycle with large buds, a G2 content of DNA, and monopolar spindles, although this phenotype can vary depending on the medium. Additionally, we describe a genetic interaction between *RPT4* and the naturally polymorphic gene *SSD1*, which in wild-type form modifies the *rpt4-145* phenotype such that cells arrest in G2 of the first cycle with complete bipolar spindles.

SELECTIVE proteolysis via the ubiquitin/proteasome pathway is fundamental to eukaryotic cell cycle progression (King *et al.* 1996; Koepp *et al.* 1999; Tyers and Jorgensen 2000). Protein degradation provides a rapid, irreversible method of inactivating regulatory molecules, including cyclins, cyclin-dependent kinase inhibitors, and anaphase inhibitors, at the appropriate time in the cycle. Ubiquitination (Ciechanover 1998; Hershko and Ciechanover 1998) targets proteins for degradation by 26S proteasomes, which are large, self-compartmentalizing proteases found in the cytoplasm and nucleus (Voges *et al.* 1999; Zwickl *et al.* 2000). Each proteasome is assembled from a barrel-shaped 20S core particle (CP) and one or two 19S regulatory particles (RPs) linked to the ends of the CP. Proteolytic activity is sequestered inside the CP, and ubiquitinated substrates are believed to be recognized, unfolded, and translocated into the CP by the RP in an ATP-requiring process.

The RP contains ~18 different subunits, 6 of which are ATPases (Ferrell *et al.* 2000). The subunits have been given a unified nomenclature that designates the 6 putative ATPases as Rpt1-6 (for regulatory particle triple-A) and the remaining subunits as Rpn1-12 (for regulatory particle non-ATPase; Finley *et al.* 1998). The RP consists of two subcomplexes, the base and the lid (Glickman *et al.* 1998a). Each RP base from *Saccharomyces cerevisiae* contains all 6 Rpt subunits assembled into a heteromeric complex (Glickman *et al.* 1998a,b), as well as Rpn1p, Rpn2p, and Rpn10p, and appears to bind directly to the CP. The lid, which is built of the remaining subunits, is located distal to the base. A chaperone-like ability to refold a denatured protein is exhibited by the base *in vitro*, suggesting that it could function *in vivo* to unfold substrates and promote their translocation into the CP (Braun *et al.* 1999). The base is also believed to play a role in opening the CP channel, which is blocked in yeast by portions of CP subunits (Groll *et al.* 1997, 2000).

The six ATPases appear to have distinct functions, since null mutations in each of the corresponding genes are lethal and the lethality is not suppressed by overproduction of other Rpt subunits (Ferrell *et al.* 2000). Experiments involving selective chemical inactivation of Rpt4/Sug2p and Rpt6/Sug1p support the idea that these subunits are nonredundant (Russell *et al.* 2001), as does the finding that analogous mutations in the ATP-binding regions of the six Rpt subunits produce distinct phenotypes (Rubin *et al.* 1998). Interestingly, Rpt2p appears to play a unique role in gating the CP

[1]*Corresponding author:* American Association for the Advancement of Science, 1200 New York Ave. NW, Washington, DC 20005. E-mail: hmcdonal@aaas.org

[2]*Present address:* Department of Biology, Hamilton College, Clinton, NY 13323.

channel (Köhler *et al.* 2001). Additionally, whereas *rpt6/cim3* and *rpt1/cim5* temperature-sensitive (ts) mutations cause cells to arrest at G2/M with a short bipolar spindle (Ghislain *et al.* 1993), a ts *rpt4/pcs1^{td}* mutation causes cells to arrest with a monopolar spindle (McDonald and Byers 1997). Thus, we previously hypothesized that Rpt4p plays a specific role in the duplication of the spindle pole body (SPB), which functions as the centrosome equivalent and serves to organize microtubule arrays in yeast (Byers 1981a).

SPB duplication is a key event in the cell cycle, essential for the formation of a bipolar spindle. Electron microscopy (EM) reveals that the SPB is a trilaminar disk embedded in the nuclear envelope throughout the cell cycle; microtubules emanate from its outer and inner surfaces into the cytoplasm and nucleus, respectively (Byers 1981a). The single SPB that is present at the beginning of the cell cycle must duplicate to generate the two poles of the bipolar spindle. The first visible sign of duplication is the appearance of the satellite early in G1. This structure appears as an aggregate of material on the cytoplasmic surface of the half-bridge, a darkly staining region of the nuclear envelope adjacent to the extant SPB. The satellite apparently matures into a larger structure, the duplication plaque (Adams and Kilmartin 1999), which becomes embedded in the nuclear envelope as a second, mature SPB later in G1. *rpt4/pcs1^{td}* cells fail to form a satellite at restrictive temperature, perhaps because they contain an abnormal half-bridge structure (McDonald and Byers 1997). Thus, these cells exhibit a failure of SPB duplication at the earliest known stage of the process. Since other early landmarks of the cell cycle (bud formation and DNA synthesis) are not prevented, we hypothesized that the Rpt4/Pcs1 subunit is specifically required for the proteolysis of substrate(s) that must be degraded for SPB duplication to occur (McDonald and Byers 1997).

To investigate the structure and function of Rpt4p further, and to determine whether additional *rpt4* mutations also affect SPB duplication, we systematically mutagenized *RPT4* and analyzed the resulting phenotypes. Primarily, we converted clustered, charged amino acids to alanine. Since such residues are likely to be found at the surface of a protein, and since the alanine side chain is small and uncharged, this method can be an effective way of subtly perturbing surface domains and protein interactions without grossly distorting protein folding (*e.g.*, Cunningham and Wells 1989; Bass *et al.* 1991; Bennett *et al.* 1991; Wertman *et al.* 1992; Reijo *et al.* 1994). We generated 53 charged-to-alanine mutations, as well as several others suggested by analysis of the Rpt4p sequence. Our results reveal an important role for the C terminus in Rpt4p function and indicate that much of the N terminus is dispensable. Phenotypic analysis of the two conditional *rpt4* mutants recovered from this screen reveals roles for *RPT4* in other aspects of early cell cycle progression, in addition to SPB duplication.

MATERIALS AND METHODS

Strains and culture techniques: All strains were of the S288C genetic background. Allele replacement was done in the haploid yeast strain Wx257-5c (*MAT***a** *ura3-52 leu2-3, 112 trp1*Δ *his3*Δ *ssd1-d*, originally constructed by Mark Winey). Strains containing the *rpt4-145* and *rpt4-150* alleles were crossed to Wx257-7b (*MAT*α *ura3-52 leu2-3, 112 trp1*Δ *ssd1-d*) to obtain *MAT*α *rpt4-145* and *MAT*α *rpt4-150* strains, which were in turn crossed to BY4741 (*MAT***a** *his3*Δ*1 leu2*Δ*0 met15*Δ*0 ura3*Δ*0 SSD1*; Brachmann *et al.* 1998) to move the *rpt4* alleles to an *SSD1* background. Standard yeast genetic methods were used (Mortimer and Hawthorne 1969) and yeast media were made as described (Hartwell 1967; Ausubel *et al.* 1994). 5-Fluoroorotic acid (5-FOA) was purchased from Toronto Research Chemicals (North York, Ontario) and cycloheximide was purchased from Sigma (St. Louis). For cell synchronization, cells were arrested with 10 μM α-factor (Sigma) and released as described (Winey *et al.* 1991). Bacterial strains DH5α, XL10-Gold (Stratagene, La Jolla, CA), and TOP10 (Invitrogen, Carlsbad, CA) were used for plasmid construction; bacterial media were made as described (Sambrook *et al.* 1989).

Plasmid construction: Plasmid pHM59 was constructed for use as a template for *RPT4* mutagenesis. It bears a 1.9-kb fragment of genomic DNA that contains the *RPT4* coding sequence, with a selectable marker (*TRP1*) inserted into the *RPT4* downstream flanking sequence. As a first step toward pHM59 construction, *TRP1* was inserted into the Wx257-5c genome 93 bp downstream of the *RPT4* stop codon using a hybrid-oligonucleotide polymerase chain reaction (PCR)-based method (Baudin *et al.* 1993). *TRP1* was amplified from pRS314 (Sikorski and Hieter 1989) using forward primer HM-100 5′ TGCGAGAAAGCTTGCCTTATTTAAGCTCGAAA TGGCTATGGAAGCATTTAATAGAACAG 3′, reverse primer HM-99 5′ AAATTTAGCTTATTGAAAAAGCATTTAGAACTA GAGTTCACAGGCAAGTGCACAAACA 3′, and the eLONGase enzyme mix (Invitrogen Life Technologies). Underlined sequences anneal to *TRP1*; the nonunderlined portions represent sequences that flank the site 93 bp downstream of the *RPT4* stop codon. The resulting product, a 975-bp *TRP1*-containing fragment flanked by *RPT4* downstream sequences, was used to transform strain Wx275-5c to Trp$^+$ by the Li-acetate method (Gietz *et al.* 1992). Amplification of genomic DNA derived from Trp$^+$ transformants using primers HM-50 (5′ CACTCGAGGAGCTATCAACGGTGGGAACT 3′, which anneals 255 bp upstream of the *RPT4* start codon) and HM-51 (5′ CACTCGAGGTTGGGATACACAGCGTGCC 3′, which anneals 373 bp downstream of the *RPT4* stop codon), indicated that the fragment had integrated at the *RPT4* locus in one case. [Insertion of *TRP1* at this position relative to *RPT4* in the Wx257-5c genome, to create strain YHM101, does not detectably affect yeast viability or growth characteristics (Figure 1, section 2).] The 2.9-kb PCR product was inserted into pCR4-TOPO (Invitrogen) to create pHM59. The *TRP1*-marked *RPT4* gene can be excised as a single fragment from the vector using *Xho*I (site underlined in primers HM-50 and HM-51 above). Restriction enzymes were purchased from New England Biolabs (Beverly, MA).

Site-directed mutagenesis and construction of deletion mutants: The desired mutations in *RPT4*, together with silent mutation(s) that either create or destroy a restriction site at or very near the codon-altering mutation(s), were generated in pHM59 using the Stratagene QuickChange method. Site-directed mutagenesis was performed according to the manu-

facturer's instructions, except that oligonucleotide primers were designed to have a melting temperature of ~70°. Oligonucleotides were synthesized by MWG Biotech (High Point, NC), Sigma-Genosys (The Woodlands, TX), and Integrated DNA Technologies (Coralville, IA); sequences are available upon request. Eight of the alleles were made by remutagenizing a previously constructed allele such that two nearby sets of mutations were combined.

Two deletions were constructed in *RPT4*. To facilitate their construction, a *Bam*HI site was engineered at position 15 (relative to the first nucleotide in the start codon) in *RPT4*. To create the first deletion (*rpt4-1*Δ), a naturally occurring *Bam*HI site at position 138 was utilized. Following digestion with *Bam*HI to release the appropriate fragment, the plasmid was reclosed such that an in-frame deletion in *RPT4* was created. To create the second, larger deletion (*rpt4-2*Δ), a *Bgl*II site in *RPT4* at position 246 was utilized, together with the engineered *Bam*HI site, in the same manner.

Sequence analysis: DNA sequence reactions were performed using the Taq DyeDeoxy Terminator cycle sequencing kit or the BigDye Terminator cycle sequencing kit (both from Applied Biosystems, Foster City, CA) and were analyzed on an ABI 310 automated sequencer (Colgate University) or on an ABI 377XL automated sequencer (University of Washington Molecular Pharmacology Facility).

Allele replacement: Following site-directed mutagenesis, plasmids were digested with *Xho*I to excise the *TRP1*-marked *RPT4* fragment. The digested DNA was transformed into strain Wx257-5c containing pHM49, a *URA3*-marked *CEN* plasmid that bears the *RPT4* coding region and sufficient flanking sequence (93 bp upstream and 102 bp downstream) to supply *RPT4* function in haploid strains containing a disrupted genomic copy of the gene (McDonald and Byers 1997). Genomic DNA was isolated from Trp^+ transformants and the *RPT4* locus was amplified using primers HM-279 (5′ CAGCTGTA CTGTCTTTGTTC 3′) and HM-280 (5′ GATTGACCACATCT TTAGGC 3′), which lie 103 bp upstream and 104 bp downstream of the transformed fragment's endpoints, respectively. A 3.2-kb product is obtained if the *TRP1*-marked fragment inserts into the *RPT4* locus, whereas a 2.2-kb product is obtained if the *RPT4* locus is unmodified. Between 20 and 90% of Trp^+ transformants were generally found to incorporate the fragment at the *RPT4* locus. Restriction analysis of PCR-amplified fragments and, in some cases, sequence analysis were then performed to test for the presence of the desired mutation(s) in the genome.

Phenotypic analysis of *rpt4* mutants: To determine the effects of the inserted mutant *rpt4* alleles in the absence of wild-type *RPT4*, strains were plated on media containing 5-FOA to select for loss of the *URA3*-marked pHM49 plasmid at 25° (Boeke *et al.* 1984). An inability to obtain 5-FOA-resistant colonies indicated that the respective mutations cause a recessive lethal (RL) phenotype. If 5-FOA-resistant colonies were obtained, they were tested on YEPD media for cold or heat sensitivity at 10° or 37.5°, respectively. At least two independent transformants were tested in this manner for each mutant allele, and following these analyses, the presence of the desired mutation in the genome was reconfirmed in each case. In two cases (*rpt4-132* and *rpt4-149*), however, Trp^+ transformants containing the constructed mutations were never recovered, although in each case 24 candidates with *TRP1* inserted downstream from *RPT4* were analyzed for the presence of the desired mutations. These mutations therefore may cause dominant lethality. To determine whether alleles causing reduced growth or temperature sensitivity were dominant or recessive, relevant strains were retransformed with pHM49 and tested for growth at 30° and 37.5°.

GFP-Rpt4-150 expression: To investigate whether the ts *rpt4-150* mutation affects the level of Rpt4p at restrictive temperature, a *LEU2*-marked *CEN* plasmid (pHM54) that encodes a green fluorescent protein (GFP)-Rpt4p fusion was used (McDonald and Byers 1997). The expression of this fusion is driven by the *RPT4* promoter. pHM54 was transformed into haploid yeast strain YHM10.1.49 (McDonald and Byers 1997), which contains a disrupted chromosomal copy of *RPT4* and is made viable by the presence of pHM49. Leu^+, 5-FOA-resistant transformants (which have lost pHM49) were found to be capable of growth at both 30° and 36.5°, indicating that the GFP-Rpt4p fusion supplies Rpt4p function at both temperatures.

The *rpt4-150* mutations were reconstructed in the pHM54 *RPT4* sequence to create pAH66. To test the functionality of this GFP-Rpt4-150 protein fusion, pAH66 was transformed into strain YHM10.1.49. In this case, Leu^+ transformants were found to be capable of growth at 30° but not at 36.5° on medium containing 5-FOA, indicating that the GFP-Rpt4-150 fusion provides Rpt4p function at low but not high temperature. Therefore, the plasmid-borne construct encoding the GFP-Rpt4-150 fusion behaves similarly to the chromosomal *rpt4-150* allele, leading to a restrictive temperature 1° lower than that of the non-GFP-fused, chromosomal allele.

Cytological techniques and Western analysis: Cells were prepared for immunofluorescence microscopy as described (Kilmartin and Adams 1984; Jacobs *et al.* 1988). Microtubules were visualized using the DM1A mouse monoclonal anti-α-tubulin antibody (Sigma) and fluorescein-conjugated goat anti-mouse IgG (Molecular Probes, Eugene, OR), both at 1:100 dilution. DNA was visualized with 4′,6-diamidino-2-phenylindole (DAPI) at 1 μg/ml (Sigma).

Cells were prepared for thin-section EM (Byers and Goetsch 1991) and flow cytometry (Hutter and Eipel 1979) as described.

Yeast cell extracts for Western analysis were prepared as follows. Cells derived from 10-ml cultures at a density of 4×10^7 cells/ml were harvested, rinsed, and resuspended in 400 μl loading buffer (125 mm Tris-Cl, pH 6.8, 20% glycerol, 4% SDS, 2% β-mercaptoethanol, 0.1% bromophenol blue) containing 2 mm Pefabloc SC (Boehringer Mannheim, Indianapolis). A total of 400 μl of glass beads (Biospec Products, Bartlesville, OK) were added to each sample, which were then alternately boiled and vortexed three times for 2 min and 30 sec, respectively. After centrifugation for 30 sec to pellet insoluble material, volumes of supernatant containing equivalent amounts of total protein (5–10 μl) were subjected to SDS-PAGE (Laemmli 1970) using a 6% polyacrylamide gel. Following transfer to nitrocellulose, GFP fusion proteins were visualized using anti-GFP antiserum (Invitrogen) followed by horseradish peroxidase-conjugated goat anti-rabbit IgG (Zymed, South San Francisco, CA), both at 1:2500 dilution. The signal was visualized using the enhanced chemiluminescence system (Amersham, Piscataway, NJ).

RESULTS

Overview: To improve our understanding of Rpt4p, we generated 58 novel *rpt4* alleles and analyzed the resulting phenotypes. Fifty-three of these alleles were constructed such that clustered, charged amino acids (Arg, Asp, Glu, His, and Lys) were converted to alanine; between one and four charged residues were mutated per variant. Several additional point mutations and deletions were made in regions of the protein with predicted structural features or functional roles (see below). The mutations are summarized in Table 1.

TABLE 1

Summary of mutations

Allele	Amino acid replacement	Detection[a]	Phenotype[b]
RPT4	None	NA	WT
*rpt4-1*Δ	Amino acids 6–46 deleted	PCR	WT
*rpt4-2*Δ	Amino acids 6–82 deleted	PCR	WT
rpt4-101	E3A, E4A	+*Bam*HI	WT
rpt4-102	H25A, E26A	+*Pvu*II	WT
rpt4-103	E36A, E37A, H38A	+*Pst*I	WT
rpt4-104	H39A, E40A	+*Pst*I	WT
rpt4-105	E41A, E42A, R45A	+*Pst*I	WT
rpt4-106	E49A, E51A	+*Bgl*I	WT
rpt4-107	E49A, E51A, D71A, D72A	+*Bgl*I, +*Pvu*II	RG[d]
rpt4-108	K63A	+*Sac*I	WT
rpt4-109	K63A, K75A	+*Sac*I, +*Pvu*II	WT
rpt4-110	E66A, H67A	+*Nhe*I	WT
rpt4-111	R68A, R69A	+*Xho*I	WT
rpt4-112	R68A, R69A, R82A, D83A	+*Xho*I, −*Xba*I	WT
rpt4-113	D71A, D72A	+*Pvu*II	WT
rpt4-114	K75A	+*Pvu*II	WT
rpt4-115	I81D	+*Pvu*I	WT
rpt4-116	R82A, D83A	−*Xba*I	WT
rpt4-117	L84E	−*Xba*I	WT
rpt4-118	E85A, K86A	+*Eae*I	WT
rpt4-119	D89A, K90A	+*Eae*I	WT
rpt4-120	D94A, K96A	+*Bgl*I	WT
rpt4-121	L98E	+*Eco*RV	WT
rpt4-122	K141A, K142A	+*Pst*I	WT
rpt4-123	K141A, K142A, D149A	+*Pst*I, +*EaeI*	RG[d]
rpt4-124	D149A	+*Eae*I	WT
rpt4-125	R161A, E162A	+*Pst*I	RL
rpt4-126	R194A, E195A	+*Pst*I	WT
rpt4-127	K213A, K216A	+*Pst*I	RL
crl13[c]	G13R, L231R	Sequence	ts
rpt4-128	D253A, K254A	+*Eae*I	WT
rpt4-129	D253A, K254A, K271A, E272A	+*Eae*I, +*Pst*I	WT
rpt4-130	R264A, E265A	+*Eae*I	WT
rpt4-131	K271A, E272A	+*Pst*I	WT
rpt4-132	H273A, E274A	+*Bgl*I	DL (?)
rpt4-133	D281A, E282A	+*Pvu*II	RL
rpt4-134	D284A	+*Eae*I	RL
rpt4-135	R289A, R290A	+*Kpn*I	RL
rpt4-136	E293A	+*Pst*I	WT
rpt4-137	R299A, E300A	+*Pst*I	RG
rpt4-138	R299A, E300A, R342A	+*Pst*I, +*Sac*I	RG[d]
rpt4-139	R329A, D331A	+*Xba*I	RL
rpt4-140	R342A	+*Sac*I	RG
rpt4-141	D344A, K346A	+*Nhe*I	WT
rpt4-142	R357A, E359A	+*Nhe*I	RL
rpt4-143	K367A, K369A	+*Pst*I	RL
rpt4-144	D375A, E377A	+*Pvu*II	RG[d]
rpt4-145	D375A, E377A, D390A, R392A	+*Pvu*II, +*Pvu*I	ts[d]
rpt4-146	K381A	+*Pst*I	WT

(*continued*)

Each mutant allele, marked with *TRP1*, was used to replace the wild-type *RPT4* gene in haploid strain Wx257-5c, which also contained a wild-type copy of *RPT4* on a *URA3*-marked plasmid. After gene replacement at the *RPT4* locus had been verified, we selected for loss of this plasmid on medium containing 5-FOA and determined the resulting phenotype (see MATERIALS AND METHODS). We recovered 51/53 of the charged-to-alanine mutant alleles *in vivo* (the remaining two may cause dominant lethality; see MATERIALS AND METHODS). Nine

TABLE 1

(Continued)

Allele	Amino acid replacement	Detection[a]	Phenotype[b]
rpt4-147	D390A, R392A	+*Pvu*I	WT
rpt4-148	E397A	+*Pst*I	WT
rpt4-149	R404A, D405A	+*Pvu*II	DL (?)
rpt4-150	D406A, R407A	+*Pst*I	ts
rpt4-151	D408A	+*Sac*I	WT
rpt4-152	D413A, D414A	+*Pst*I	RL
rpt4-153	R420A, K421A	+*Pst*I	WT
rpt4-154	E424A	+*Pst*I	WT
rpt4-155	E424A, E433A	+*Pst*I, +*Pvu*I	WT
rpt4-156	E433A	+*Pvu*I	WT

[a] Restriction sites that were either created (+) or destroyed (−) in the mutant allele are indicated.
[b] WT, wild type; RG, reduced growth, particularly at high temperature; ts, temperature sensitive; RL, recessive lethal; DL, dominant lethal.
[c] James Haber (Brandeis University).
[d] The RG and ts alleles indicated display mild semidominance. All other RG and ts alleles are recessive.

of the alleles cause RL phenotypes, whereas most (34) of the remaining alleles appear to result in wild-type (WT) phenotypes. Figure 1, section 3, shows *rpt4-129*, a representative WT strain, compared to the parent, Wx257-5c (Figure 1, section 1), or to its WT derivative, YHM101, which has incorporated the *RPT4*::*TRP1* fragment at the *RPT4* locus (Figure 1, section 2). Six alleles cause reduced growth (RG), especially at elevated temperature (37.5°); representative strains *rpt4-123* and *rpt4-137* are shown in sections 4 and 5. Two strains, *rpt4-145* (Figure 1, section 6) and *rpt4-150* (Figure 1, section 7), are ts, but none were found to be cold sensitive. Finally, because *RPT4* was originally identified as the cycloheximide-resistant, ts lethal allele *crl13* (McCusker and Haber 1988; section 8 in our Figure 1), we tested each of the strains for resistance to 1 μg/ml cycloheximide; none were found to be resistant (data not shown).

Mutational analysis of the N terminus: The N-terminal region of Rpt4p contains a very hydrophilic region (residues 13–96 are 49% charged, 77% charged and polar), a putative bipartite nuclear localization signal (NLS; residues 62–78), and a region (residues ~69–101) that is predicted to participate in the formation of a short α-helical coiled-coil (Figure 2). We hoped to gain insight into the functional significance of these features with our mutational analysis.

We constructed a total of 21 point mutations or clusters of mutations in the N-terminal region (Table 1) and determined that 20 of them resulted in no detectable mutant phenotype. (The *rpt4-107* allele confers a mild RG phenotype.) The ability of Rpt4p to function despite these mutations suggests that the N-terminal region, which represents the most divergent region of Rpt4p relative to other Rpt subunits (Figure 3), might be dispensable for function. To test this idea, we created two alleles, *rpt4-1*Δ and *rpt4-2*Δ, which are deleted for residues 6–46 and residues 6–82, respectively. Strains containing these alleles again display a WT phenotype, indi-

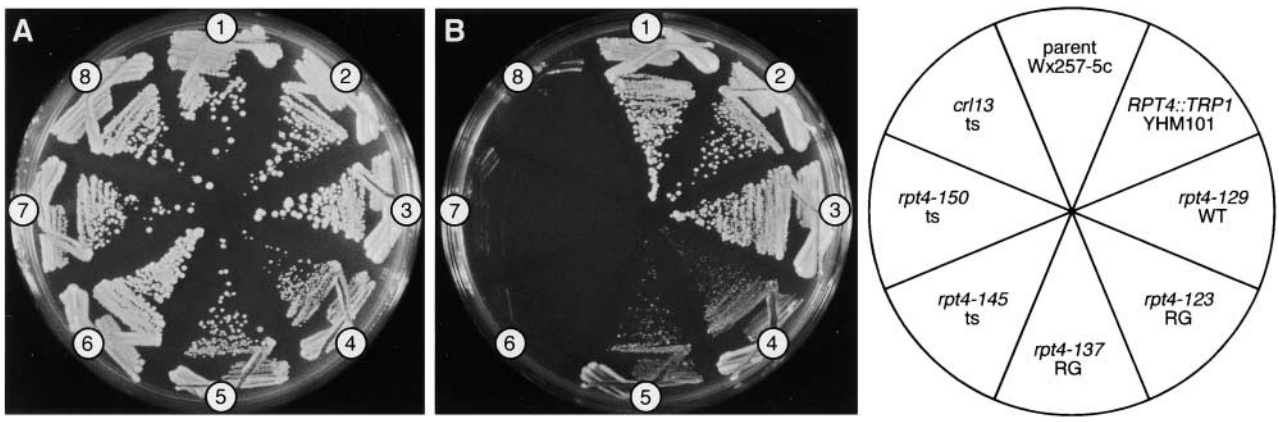

Figure 1.—Growth characteristics of strains carrying selected *rpt4* alleles. Duplicate plates were grown at 30° (A) or at 37.5° (B). Sections: 1, parental haploid strain Wx257-5c; 2, *TRP1*-marked strain YHM101; 3, representative WT strain *rpt4-129*; 4 and 5, representative RG strains *rpt4-123* and *rpt4-137*; 6, ts strain *rpt4-145*; 7, ts strain *rpt4-150*; 8, *crl13* (McCusker and Haber 1988).

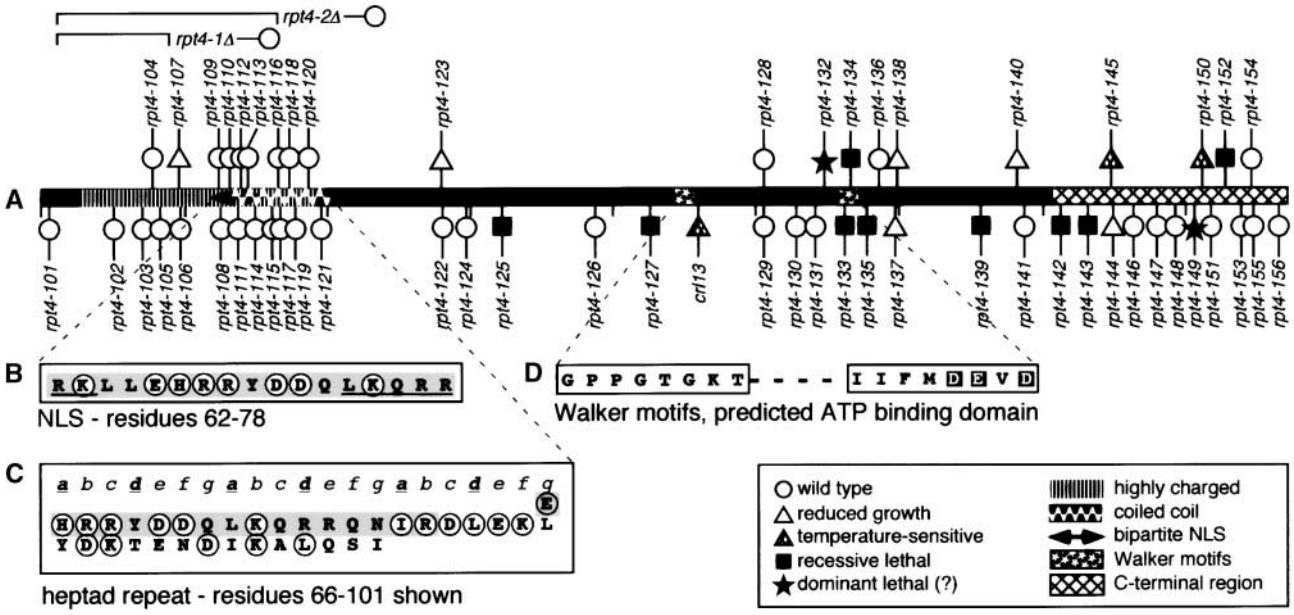

FIGURE 2.—Rpt4p structural features and mutations. (A) Schematic representation of Rpt4p. The highly charged N-terminal region is represented by a striped bar, the predicted bipartite NLS by a double-headed arrow, the predicted coiled-coil domain (which partially overlaps the NLS) by a white wave pattern, the Walker motifs (which form the predicted ATP binding domain) by a star pattern, and the C-terminal region by a hatched bar. The location of each (set of) mutation(s) is indicated at the appropriate position on the Rpt4p sequence. Associated phenotypes are symbolized by open circles (WT), open triangles (RG), hatched triangles (ts), solid squares (RL), or solid stars (presumptive DL). The extent of the two deletions is indicated above the Rpt4p diagram. (B) Predicted bipartite NLS. These signals have a consensus pattern of 2 basic residues, a 10-residue spacer and a second region containing at least 3 basic residues out of 5 (ROBBINS *et al.* 1991). Residues in the two basic regions are underlined. Residues that were mutated are circled; all residues in the NLS were deleted in *rpt4-2*Δ (symbolized by the shaded bar). (C) Heptad repeat (diagrammed *a b c d e f g*) that is predicted to participate in coiled-coil formation by the program COILS, version 2.1 (LUPAS *et al.* 1991; MTIDK matrix used and positions *a* and *d* weighted 2.5-fold). The N-terminal endpoint of the coil region is predicted to be position 66 if a 28-residue window is used and position 69 if a 21-residue window is used. Residues that were mutated are circled, and the portion of this region that is deleted in *rpt4*-2Δ is indicated by a shaded bar. (D) Walker motifs A and B. Residues that were mutated in the second motif are indicated by solid squares.

cating that these residues play no essential role in Rpt4p function. As well as deleting a significant portion of the hydrophilic region, *rpt4-2*Δ also removes the potential NLS and half of the putative coil region.

Mutational analysis of the ATPase domain: The six putative ATPases of the proteasome RP are members of the AAA protein family, a group of ATPases that contain Walker A and B motifs characteristic of ATP-binding domains (WALKER *et al.* 1982) within an extended, conserved region of ~230–250 residues known as the AAA cassette (KUNAU *et al.* 1993; BEYER 1997). The region of highest sequence identity [~60% in pairwise comparisons using the BLAST alignment program (ALTSCHUL *et al.* 1990)] in the Rpt subunits corresponds to regions D–H of the AAA cassette (BEYER 1997) and is defined by residues 213–352 in Rpt4p (Figure 3). Mutations in this region are much more likely to be deleterious than mutations in the N-terminal region. Of the 14 recovered charged-to-alanine mutations in the central region, 5 were determined to be RL. (An additional RL allele, *rpt4-125*, affects residues that lie in region A of the AAA cassette.) Four of the RL alleles affect residues either within or very near Walker motifs A and B (Figure 2). *rpt4-132*, which also affects residues located very near Walker motif B, represents one of the two alleles we were not able to recover *in vivo*, suggesting that it may exert a dominant lethal (DL) effect. None of the mutations we constructed in this region resulted in a ts phenotype, but we sequenced the previously identified *crl13* allele (MCCUSKER and HABER 1988) and determined that it contains two changes (G13R and L231R) compared to wild type. Given that residues 6–82 can be deleted from Rpt4p without discernible effect, the ts effect of the *crl13* allele most likely derives from the L231R mutation. This conserved leucine residue is separated from Walker motif A by one residue. The remaining 9 mutations in the central region caused either RG or WT phenotypes (Table 1). Many of these mutations affect conserved residues (Figure 3).

Mutational analysis of the C terminus: We define the C terminal region of Rpt4p as residues 353–437 because this portion shows reduced conservation compared to the central ATPase region [~31% identity in pairwise BLAST comparisons (ALTSCHUL *et al.* 1990)] among Rpt subunits (Figure 3). Although it contains no previously characterized motifs or predicted structural features,

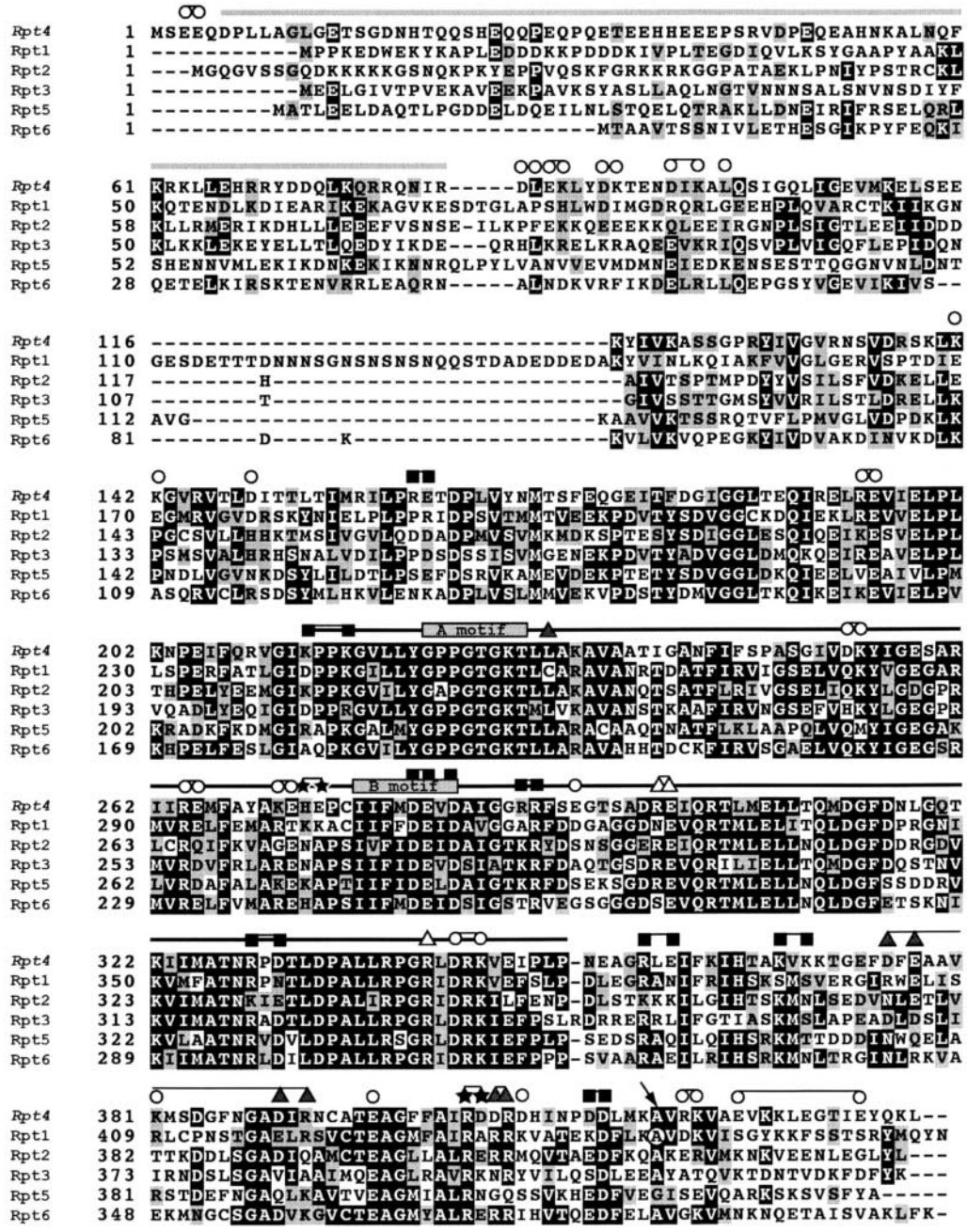

FIGURE 3.—Multiple sequence alignment of the *S. cerevisiae* Rpt proteins. Solid boxes represent amino acid identity and shaded boxes represent similarity. The shaded line above the alignment indicates the region of Rpt4p that was deleted in the *rpt4*-2Δ allele, whereas the solid line above the alignment indicates regions D–H of the AAA cassette, the region of highest similarity between the six proteins. This region contains Walker motifs A and B, indicated by shaded boxes. Positions and phenotypes of *rpt4* mutations are symbolized by open circles (WT), open triangles (RG), shaded triangles (ts), and solid squares (RL). Lines connecting two symbols indicate that both positions are mutant in one allele. The locations of two mutations that could not be recovered *in vivo* are indicated by solid stars. Symbols depicting mutations that fall in the deleted region of *rpt4-2*Δ have been omitted for simplicity. An arrow indicates the location of the *RPT1* mutation that is synthetic lethal with a mutation in *RPN12* (TAKEUCHI and TOH-E 1999). The program BOXSHADE (http://www.ch.embnet.org/software/BOX_form.html) was used to create this display.

mutations we generated reveal that the C-terminal region of Rpt4p is quite important for its function. One of the two potential DL alleles (*rpt4-149*) that we were unable to recover *in vivo* affects residues in this region. Of the 14 recovered mutations, 3 were RL (*rpt4-142*, *rpt4-143*, and *rpt4-152*); all of these affect at least one conserved residue (Table 1, Figure 3). One allele (*rpt4-144*) causes a RG phenotype. Additionally, the only ts lethal mutations generated by this mutagenesis are found in this region: *rpt4-145* (D375A, E377A, D390A, R392A) and *rpt4-150* (D406A, R407A). The *rpt4-145* strain has a restrictive temperature (36°) slightly lower than that of *rpt4-150* (37°–37.5°). The remainder of our analyses focused on these two alleles.

We wished to determine whether the ts mutants *rpt4-145* and *rpt4-150* exhibit defects similar to our previously characterized *rpt4* mutant (*rpt4/pcs1*^{td}), which displays a specific failure in SPB duplication. Primarily in the second cycle after a shift to high temperature, the *rpt4/pcs1*^{td} strain arrests as large-budded cells with monopolar spindles and duplicated, unsegregated DNA (MCDONALD and BYERS 1997). To ascertain whether the *rpt4* ts alleles cause arrest at a specific stage of the cell cycle, asynchronous liquid cultures of *rpt4-145* and *rpt4-150* were shifted to 36° or 37.5°, respectively. After ~7 hr at restrictive temperature, ~80% of cells from both strains were found to be large budded, compared to 25–30% for the cultures grown at 30° (data not shown). Experi-

ments using synchronous, α-factor-arrested cultures released into fresh YM-1 media (a buffered version of YEPD) at 37° revealed that the majority of cells arrest in the second cycle after the temperature shift.

Potential genetic interaction with *SSD1*: Further characterization of the *rpt4* cell cycle arrest revealed different cell cycle behaviors (see below), depending on the strain background. One possible explanation for this observation is that the *rpt4* phenotypes might vary depending on the state of the naturally polymorphic gene *SSD1* (Sutton *et al.* 1991), which has been shown, in wild-type form, to suppress numerous different mutations (discussed in Doseff and Arndt 1995; Uesono *et al.* 1997; Kaeberlein and Guarente 2002), indicating involvement in a variety of processes. For example, *SSD1* suppresses the lethality of a *cln1 cln2* double mutation in a W303 strain background, which carries an *ssd1-d* allele (Cvrcková and Nasmyth 1993). To determine which *SSD1* allele is present in the *rpt4* strains, we amplified and sequenced the gene and found a C2094G mutation in *SSD1*, which converts Tyr698 to a stop codon. The premature truncation occurs in approximately the middle of the 1250-residue wild-type Ssd1 protein and is in accordance with the finding that an 83-kD protein is detected with anti-Ssd1p antibodies in W303 (*ssd1-d2*), whereas an essentially full-length protein is ~160 kD (Uesono *et al.* 1997). We therefore conclude that the *rpt4* strains carry an *ssd1-d* allele. For comparative purposes, we created *rpt4-145 SSD1* and *rpt4-150 SSD1* strains and performed analyses on both sets of strains in parallel, as described below.

Flow cytometry analysis: To determine whether DNA synthesis is complete at the time of *rpt4-145* and *rpt4-150* arrest, we performed flow cytometry experiments. Cells were initially grown at 30°, arrested in G1 with α-factor, and then released into fresh media (YEPD) without α-factor at 37°. Cytometry profiles taken at time points after the temperature shift are shown in Figure 4A and indicate that both *rpt4-145* and *rpt4-150* arrest with a 2N (G2) content of DNA, regardless of the *SSD1* allele present in the strain (6 hr at restrictive temperature, columns b, c, and d in Figure 4A, and data not shown). The kinetics of DNA synthesis and budding differed for the *rpt4* strains, however, depending on the *SSD1* allele present. Both *rpt4-145 ssd1-d* (column d in Figure 4A) and *rpt4-150 ssd1-d* (not shown) display a significant lag phase prior to beginning DNA synthesis; this lag phase is completely (*rpt4-145*, column c in Figure 4A) or nearly (*rpt4-150*, column b in Figure 4A) abolished in the presence of *SSD1*.

Because *SSD1* interacts genetically with genes involved in the protein kinase C pathway (see Kaeberlein and Guarente 2002 and references therein), which functions in maintaining cellular integrity in response to low osmolarity (Heinisch *et al.* 1999), we tested whether osmotic stabilization would affect the behavior of *rpt4 ssd1-d* strains. Interestingly, the addition of 0.5 M KCl to the growth medium resulted in DNA synthesis with essentially wild-type kinetics for both *rpt4-145 ssd1-d* (column e in Figure 4A) and *rpt4-150 ssd1-d* (not shown), suggesting that osmotic constraints indeed caused the lag phases. Similarly, the *rpt4 ssd1-d* strains display a delay in budding and bud growth after release from α-factor compared to *ssd1-d*, *SSD1*, or *rpt4 SSD1* strains (but similar budding behavior compared to an *rpt4-145 ssd1::LEU2* strain; not shown), which can be rescued by the addition of 0.5 M KCl to the growth medium (Figure 4B and not shown). Finally, we note that the presence of the *ssd1-d* allele in the *rpt4* strains is also associated with decreased viability after shift to high temperature (Figure 4C and not shown).

Cytological analysis: To examine the appearance of the microtubule cytoskeleton and DNA in the ts strains held at restrictive temperature, we visualized these structures using fluorescence microscopy. After ~7 hr at restrictive temperature, the DNA was unsegregated and localized adjacent to the bud neck in ~80% of the large-budded cells for both *rpt4-145 ssd1-d* and *rpt4-150 ssd1-d* (Figure 5, B and C). Large-budded wild-type cells (parental strain Wx257-5c) with DNA localized adjacent to the bud neck contain short intranuclear spindles (Figure 5A), visualized as a bright band of tubulin staining running across the nucleus. Short intranuclear spindles are characteristic of cells in G2 phase or mitotic metaphase. In contrast, the large-budded *rpt4-145* or *rpt4-150* cells rarely appeared to contain such spindle structures; few, if any, intranuclear microtubules were visible. Instead, a bundle of cytoplasmic microtubules was generally seen to extend away from the nucleus (Figure 5, B and C). Such a staining pattern is reminiscent of the monopolar spindles formed in the *rpt4/pcs1^{td}* mutant (McDonald and Byers 1997).

To determine whether the *rpt4-145* and *rpt4-150* mutations indeed result in a monopolar arrest, we used serial section EM to examine the effects of these mutations in both *ssd1-d* and *SSD1* backgrounds. In all cases, cells were initially synchronized by arrest with α-factor, after which they were released into fresh media at the restrictive temperature. We initially examined these strains after growth in YM-1 media, which generally results in better EM fixation; later experiments were done using YEPD after we observed differences in the arrest depending on the medium used.

Both *rpt4-150 ssd1-d* and *rpt4-150 SSD1* cells arrest with monopolar spindles: When grown in either YEPD or YM-1, *rpt4-150 ssd1-d* cells primarily arrest as large-budded cells during the second cell cycle (as determined by monitoring budding) after shift to high temperature. The cells do not reach G2 of the second cell cycle until 6–8 hr after the temperature shift, whereas wild-type cells reach that point by 2.5–3 hr after the shift. After 7 hr at 37.5° in YM-1, we found that the majority (33/42 or 79%) of the *rpt4-150 ssd1-d* cells had monopolar spindles (Figure 6A), indicating that the process of SPB

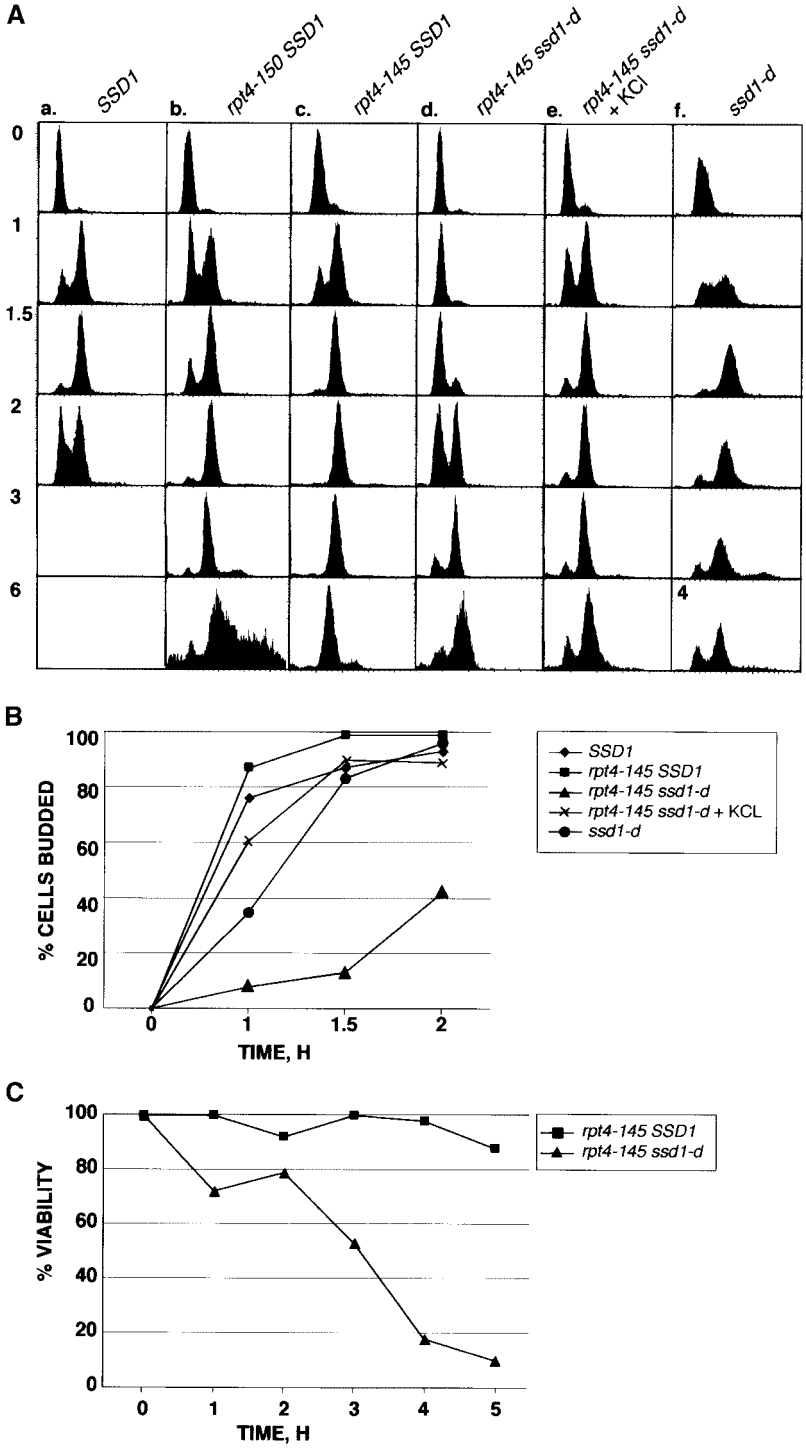

FIGURE 4.—Characterization of *rpt4-145* and *rpt4-150* strains. (A) Flow cytometric analysis. Time (in hours) after release from α-factor and shift to restrictive temperature (37°) is shown in the left column. In each histogram, the *y*-axis indicates the relative number of cells and the *x*-axis indicates the relative DNA content, determined by propidium iodide fluorescence. The left peak represents cells with a G1 content of DNA and the right peak represents cells with a G2 content of DNA. (B) The kinetics of budding for the indicated *rpt4-145* strains after release from α-factor and shift to restrictive temperature. (C) The viability of *rpt4-145* cells after release from α-factor and shift to restrictive temperature.

duplication had failed. For comparison, a normal, bipolar spindle (with SPBs found in adjacent sections) is shown in Figure 6, B and B′. Normal half-bridge structures were generally observed adjacent to the unduplicated SPBs (arrow, Figure 6A), but in no cases were satellites observed on the half-bridges. In addition to the cells displaying monopolar arrest, 7/42 (17%) had duplicated their SPBs and contained bipolar spindles. In three of these cases, imbalance in the size of the SPBs was observed, in that one SPB appeared to be about half the size of the other SPB and appeared to nucleate fewer microtubules (Figure 6C), suggesting a defect in SPB assembly or maintenance. We refer to spindles organized in such a manner as imbalanced. Similarly, we found that in YEPD, ~60% of the cells slowly traverse the first cycle after the temperature shift and arrest at G2 of the second cycle. After 6.5 hr at 37.5°, 29/37 (78%) large-budded cells examined contained monopolar spindles.

The *rpt4-150 SSD1* strain behaved similarly to *rpt4-150*

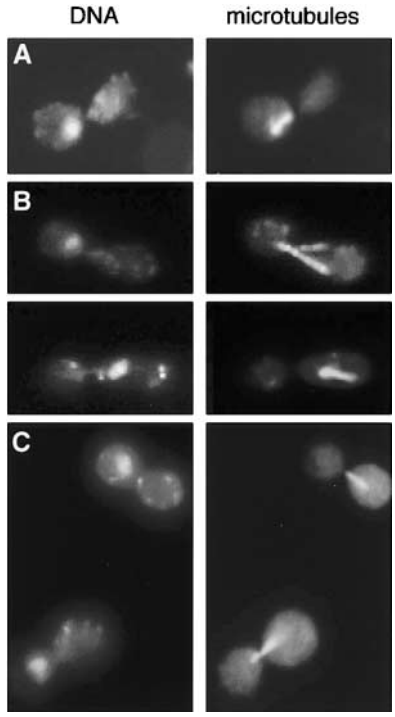

FIGURE 5.—Cytological analysis of ts *rpt4* strains using immunofluorescence microscopy. The left column shows DNA staining (DAPI) and the right column shows tubulin staining (FITC). (A) Parental strain Wx257-5c (*RPT4*). (B) *rpt4-145 ssd1-d*. (C) *rpt4-150 ssd1-d*. After transfer to restrictive temperature (37.5°), *rpt4-145 ssd1-d* and *rpt4-150 ssd1-d* cells appear to lack the intranuclear spindles that are seen in large-budded WT cells.

ssd1-d in that ~60% of the cells traverse the first cell cycle and arrest in the second cycle in YEPD. After 6 hr at 37°, 3/33 (9%) large-budded cells examined contained complete spindles, one imbalanced, whereas the majority (30/33 or 91%) contained monopolar spindles. Thus, the *SSD1* allele does not prevent the SPB duplication defect observed in *rpt4-150 ssd1-d* cells, although it does suppress the delay in DNA synthesis and budding that occurs in these cells. The unduplicated SPBs were generally associated with what appears to be an unusually curved, elongated half-bridge. This aberrant structure (indicated by the arrow, Figure 6D′) is always observed in an adjacent section in the series relative to the unduplicated SPB itself (Figure 6D). Satellites were not observed associated with these half-bridge structures, which appear similar to those seen in *rpt4/pcs1^{td}* cells (McDONALD and BYERS 1997). Although unduplicated SPBs associated with elongated half-bridges were also observed in *rpt4-150 ssd1-d* cells after growth in YEPD medium, they were not generally observed in that strain after growth in YM-1.

***rpt4-145 ssd1-d* cells arrest with monopolar spindles or imbalanced spindles depending on the growth medium:** EM analysis of the *rpt4-145 ssd1-d* strain grown in YM-1 revealed that this mutant, which arrests primarily in the second cell cycle after shift to restrictive temperature, displays a relatively uniform arrest. After incubation at 37° for 8 hr, 32/34 (94%) of the cells examined contained monopolar spindles. The unduplicated SPBs were generally associated with the elongated half-bridge described above (not shown, but similar to that shown in Figure 6, D and D′). *rpt4-145 ssd1-d* cells grown in YEPD medium, which is unbuffered, appear to be more compromised, in that they arrest primarily in G2 in the first cell cycle following the shift to high temperature and display a less uniform phenotype. Such differences have been observed in other cases; for example, *apc1-1* cells also arrest in G2 during the first cell cycle after shift to high temperature if grown in YEPD and during the second cell cycle if grown in YM-1 (L. GOETSCH, unpublished observations). After 3 hr at 37° (a time point at which these cells are still in the first cell cycle; see Figure 4A), we observed a mixture of phenotypes, including monopolar spindles and imbalanced spindles (the most common phenotype). Figure 6, F and F′, show two adjacent sections of a cell that appears to contain a broken spindle, with SPBs that are dramatically different in size and appear to nucleate different numbers of microtubules. A minority of cells contained duplicated, unseparated SPBs of unequal size (Figure 6E; arrow indicates smaller SPB).

***rpt4-145 SSD1* cells rapidly arrest with complete bipolar spindles:** During growth in YEPD medium, almost all (90%) of the *rpt4-145 SSD1* cells arrest as large-budded cells during the first cell cycle after the shift to restrictive temperature. In striking contrast to *rpt4-145 ssd1-d*, virtually all cells arrest with complete bipolar spindles ($N = 19$ and 10, after 2.5 or 5.5 hr at 37°, respectively). Very few abnormalities were observed in these spindles and the SPBs were essentially always of equal size (not shown, but similar to the spindle shown in Figure 6, B and B′). These results indicate that *SSD1* prevents the defects in SPB duplication that occur in *rpt4-145 ssd1-d* cells, in addition to essentially eliminating the delays in budding and initiation of S phase that occurs in these cells.

Rpt4-150 protein expression: The EM analysis described above reveals that the *rpt4-145* and *rpt4-150* phenotypes display some similarity to that conferred by the *rpt4/pcs1^{td}* allele (McDONALD and BYERS 1997). This allele was constructed as a degron-*RPT4/PCS1* fusion; the degron unit functions as a heat-inducible degradation signal that is degraded at high temperature, together with sequences fused downstream of it (DOHMEN *et al.* 1994). Presumably, therefore, the *rpt4/pcs1^{td}* phenotype results from a lack of Rpt4p at the restrictive temperature (although this was never proven directly). To investigate whether the *rpt4-150* mutation affects the level of Rpt4p at restrictive temperature, we utilized two plasmids: pHM54, which encodes a GFP-Rpt4p fusion that is functional at both 30° and 36.5°, and pAH66, which encodes a GFP-Rpt4-150p fusion (engineered to contain the *rpt4-*

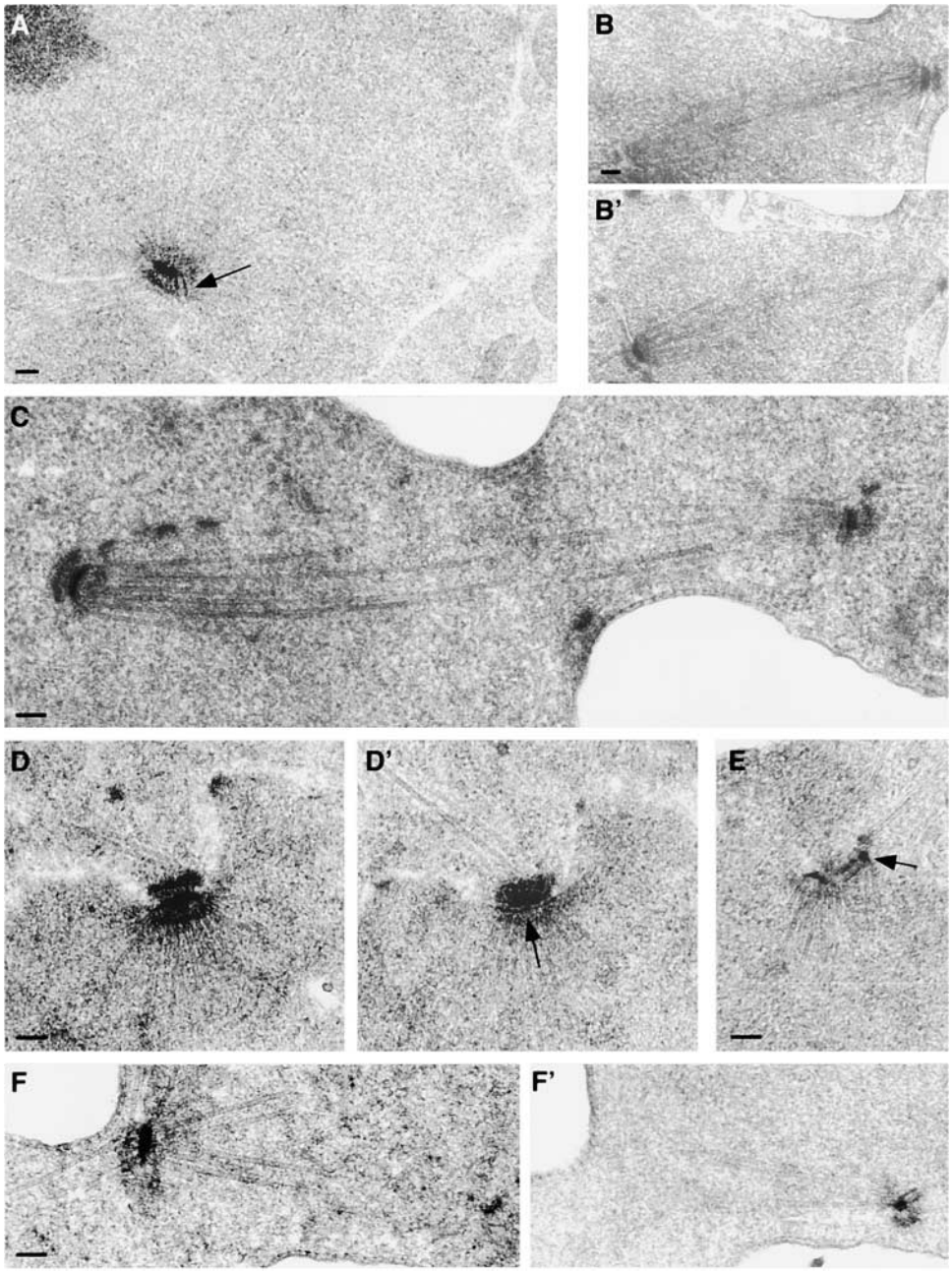

FIGURE 6.—Electron micrographs of ts *rpt4* strains after growth at restrictive temperature. (A) A monopolar spindle from an *rpt4-150 ssd1-d* cell; the arrow indicates the half-bridge structure found next to the SPB. (B and B′) Adjacent sections through an *rpt4-150 ssd1-d* cell containing a normal bipolar spindle. The two SPBs are of equivalent size; one is visible in each section. (C) A complete imbalanced spindle from an *rpt4-150 ssd1-d* cell. (D and D′) Adjacent sections from an *rpt4-150 SSD1* cell containing a monopolar spindle. A curved, half-bridge-like structure, associated with the unduplicated SPB in D, is indicated by the arrow in D′. (E) Side-by-side SPBs, which are highly imbalanced in size, from an *rpt4-145 ssd1-d* cell. The small SPB, from which microtubules appear to emanate, is indicated by the arrow. (F and F′) Adjacent sections from an *rpt4-145 ssd1-d* cell. Again, the two SPBs are imbalanced in size and the spindle appears to be broken. Bars, 0.1 μm.

150 mutation) that is functional at 30° but not at 36.5° (see MATERIALS AND METHODS).

We determined the relative amounts of Rpt4p produced by strains containing pHM54 (YHM10.1.54) and pAH66 (YHM10.1.66) after growth at 30° and 36.5° for 6 hr. Equivalent amounts of whole-cell lysates from these strains were subjected to SDS-PAGE and blotted to nitrocellulose. The blot was probed with anti-GFP antibodies, which recognize a primary band of the expected size for the GFP-Rpt4p fusion (~76 kD) in the lysates derived from strains YHM10.1.54 (Figure 7, lanes 2 and 5) and YHM10.1.66 (lanes 3 and 6). No band is detected in lysates derived from the control strain (Wx257-5c), which does not contain a GFP-Rpt4p encoding plasmid (lanes 1 and 4). Lysates run in lanes 1–3 were obtained from cells grown at 30° and those run in lanes 4–6 from cells grown at 36.5°. Approximately equivalent levels of GFP-Rpt4 and GFP-Rpt4-150 protein fusions were observed at both 30° and 36.5°. Although we were unable to obtain a functional GFP fusion with *rpt4-145* to repeat this analysis for that allele, the results with *rpt4-150* indicate that the arrest caused by at least one of the C-terminal mutations does not derive from an absence of Rpt4p at restrictive temperature.

DISCUSSION

We undertook a systematic mutagenesis of *RPT4* that focused on converting clustered, charged residues to alanine. One result to emerge from this study is that

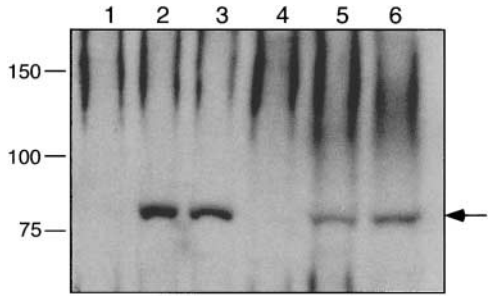

Figure 7.—Expression levels of GFP-Rpt4p fusions. Cell lysates derived from strains Wx257-5c (Rpt4p, lanes 1 and 4), YHM10.1.54 (GFP-Rpt4p, lanes 2 and 5), and YHM10.1.66 (GFP-Rpt4-150p, lanes 3 and 6) were probed using an anti-GFP antibody. Lysates shown in lanes 1–3 were derived from cells grown at 30°; those shown in lanes 4–6 were from cells grown at 36.5°. Products of the size (~76 kD) expected for a GFP-Rpt4p fusion are indicated by the arrow; size markers are in kilodaltons.

the N-terminal region of Rpt4p is quite resistant to the effects of such mutations. Like Rpt4p, the other Rpt subunits contain stretches of sequence near their N termini that are predicted to participate in α-helical coiled-coil formation (*e.g.*, see Richmond *et al.* 1997). Intersubunit coiled-coil formation has been proposed to mediate the specific pairwise interactions between Rpt subunits (which might function in the assembly of the RP) that have been observed using *in vitro* assays (Richmond *et al.* 1997). In support of this hypothesis, deletion experiments show that the N-terminal region of Rpt2/S4 is necessary and sufficient for its interaction with Rpt1/S7 *in vitro* (Richmond *et al.* 1997). However, our mutational analysis suggests that the Rpt4p coil region may not play a critical role in its function. Half of the five heptad repeats in the coiled-coil motif can be deleted (*rpt4-2*Δ) without discernible effect. Furthermore, strains containing the *rpt4-115* (I81D), *rpt4-117* (L84E), and *rpt4-121* (L98E) alleles, which convert hydrophobic residues at position *a* or *d* to charged residues and may thereby disrupt coiled-coil formation (Flemington and Speck 1990; Hu *et al.* 1990; Pellegrino *et al.* 1997), also result in WT phenotypes. Whereas, by the COILS program (Lupas *et al.* 1991), the wild-type region is given a probability near 1.0 of participating in coiled-coil formation, the I81D change in particular dramatically reduces the probability (to ~0.3).

The sequence encoding the putative bipartite NLS is also deleted in the functional *rpt4-2*Δ allele. In higher eukaryotic cells, GFP-tagged proteasomes have been detected in the cytoplasm and nucleus and enter the nucleus either during reassembly of the nuclear envelope following mitosis or via unidirectional transport across the nuclear membrane (Reits *et al.* 1997). In yeast, there is some ambiguity about proteasome localization. We previously detected nuclear localization of a GFP-Rpt4p fusion (McDonald and Byers 1997). In a different study, however, both a CP subunit and an RP subunit were detected primarily in the nuclear envelope-rough endoplasmic reticulum membrane network in *S. cerevisiae* (Enenkel *et al.* 1998). In *Schizosaccharomyces pombe*, Wilkinson *et al.* (1998) have localized 26S proteasome subunits specifically to the inner face of the nuclear envelope. These authors suggest that our observation of whole nuclear localization of a GFP-Rpt4p fusion may have been a result of its plasmid-based expression, although a more recent study, in which tagged subunits (including Rpt4/Sug2p) were encoded by chromosomal alleles, also found general nuclear localization (Russell *et al.* 1999b). In any case, the potential NLS of Rpt4p is not required for its function, nor presumably for its localization, although the latter point remains to be determined. In the absence of such a signal, Rpt4p may be recruited to the nucleus via interactions with other subunits.

We previously hypothesized that Rpt4p might mediate the degradation of distinct substrates, such as inhibitors of SPB duplication. Our hypothesis was based on the observation that strains containing the *rpt4/pcs1*^{td} allele arrest as large-budded cells with monopolar spindles at restrictive temperature (McDonald and Byers 1997). This phenotype differs markedly from that seen in strains containing conditional *rpt6/cim3* or *rpt1/cim5* mutations, which cause cells to arrest with short, bipolar spindles (Ghislain *et al.* 1993). Phenotypic analysis of strains containing the C-terminal *rpt4-145* and *rpt4-150* mutations supports a role for the Rpt4p C terminus in SPB duplication and in other aspects of G1/S progression. Although the nature of that role is unknown, one possibility is that this region interacts with specific substrate(s), which potentially include inhibitors of SPB duplication, as they are translocated into the proteasomal core. This idea contradicts the "helix shuffle" model (Rechsteiner *et al.* 1993), in which the coiled-coil regions of different Rpt subunits are postulated to interact with similar regions of distinct substrates targeted for degradation. In agreement with this model, it has been shown that murine Rpt6/Sug1p and c-Fos interact through their respective leucine zipper/coiled-coil regions and that c-Fos is present in 26S proteasomes, suggesting that Rpt6/Sug1p might function in the degradation of c-Fos (Wang *et al.* 1996). The N-terminal mutations in Rpt4p described in the present study argue against such a role for the Rpt4p coil region.

A mutation that affects the C-terminal region of Rpt1p has been shown to be synthetic lethal in combination with a mutation in *RPN12* (Takeuchi and Toh-e 1999). The mutation results in an A446V change, affecting a conserved residue (Figure 3, arrow) near the position that is mutated in the *rpt4-150* allele. It is possible that the A446V mutation identifies a region of Rpt1p that interacts with Rpn12p (Takeuchi and Toh-e 1999). By analogy, a comparable region in the C terminus of Rpt4p might interact with a different lid component,

and disruption of this interaction might result in the defects observed in the *rpt4-145* and/or *rpt4-150* strains.

Further insight into the structure/function relationship of Rpt4p should come from the analysis of additional conditional alleles. For example, it will be interesting to determine whether mutations in the ATPase domain ever lead to defects in SPB duplication and other aspects of G1/S progression. The *crl13* allele (McCusker and Haber 1988) contains such a mutation. Our preliminary analysis indicates that at the restrictive temperature, the *crl13* strain arrests as large-budded cells with short, bipolar spindles. The *SSD1* allele present in the *crl13* strain is not known, and we do not yet know whether this phenotype will vary depending on the status of *SSD1*. If *crl13* causes a bipolar spindle arrest under all conditions, this finding would support the idea that the structural features of Rpt4p required for SPB duplication map to the C-terminal region.

Although we have hypothesized that the SPB duplication and other defects in *rpt4* mutants ultimately derive from deficient proteolysis, recent evidence suggests that RP subunits function in additional, nonproteolytic roles. For example, a direct role in transcription is indicated by the finding that the RP base is recruited to an activated promoter (Gonzalez *et al.* 2002). The 19S RP (but not the 20S CP) has also been implicated in transcription elongation (Ferdous *et al.* 2001) and in the regulation of nucleotide excision repair (NER), a role that appears to be modulated by the NER protein Rad23 (Russell *et al.* 1999a; Gillette *et al.* 2001). Although the exact function of the RP in these processes is unknown, one possibility is that the chaperone-like activity of the RP base (Braun *et al.* 1999) acts in the assembly or disassembly of NER machinery (Russell *et al.* 1999a; Gillette *et al.* 2001). The SPB duplication defect in *rpt4* mutants might reflect loss of this chaperone-like activity, for example, rather than defective proteolysis.

RAD23 has a redundant function in SPB duplication, in addition to its role in NER. Specifically, *dsk2*Δ *rad23*Δ double mutants display a ts failure in SPB duplication (Biggins *et al.* 1996). We have also observed genetic interactions among *dsk2*Δ, *rad23*Δ, and *rpt4-145*. While neither *rad23*Δ nor *dsk2*Δ single mutations are ts, *rad23*Δ *rpt4-145* and *dsk2*Δ *rpt4-145* strains arrest as large-budded cells with a G2 content of DNA ~2.5 hr after shift to 37° (YEPD medium). These cells arrest with monopolar spindles (100% for *dsk2*Δ *rpt4-145* and 62% for *rad23*Δ *rpt4-145*) in an *ssd1-d* background and with complete bipolar spindles (100% for each strain) in an *SSD1* background (L. Goetsch, unpublished observations). Further work is needed to define the functional relationship of these proteins in cell cycle progression.

Additional work is also required to determine the nature of the relationship between *SSD1* and *RPT4*. The function of Ssd1p is unknown, although it has been shown to bind RNA and is localized primarily in the cytoplasm (Uesono *et al.* 1997). *SSD1* prevents the delays in DNA synthesis and budding seen in both *rpt4 ssd1-d* mutants and dramatically modifies the *rpt4-145 ssd1-d* phenotype (monopolar or imbalanced spindle arrest) such that *rpt4-145 SSD1* cells arrest at G2/M with short bipolar spindles during the first cycle at restrictive temperature. This finding reveals a role for Rpt4p at a second point in the cell cycle, perhaps similar to that seen for Rpt1/Cim5p and Rpt6/Cim3p. The ability of *SSD1* to modify the *rpt4* phenotypes appears to derive at least partially from its role in the maintenance of cellular integrity, which it promotes in parallel with the protein kinase C pathway (see Kaeberlein and Guarente 2002). The observation that osmotic stabilization can rescue the delays in DNA synthesis and budding in *rpt4 ssd1-d* strains, as does *SSD1*, supports this idea. Defective cellular integrity does not appear to explain the origin of the SPB duplication defects in *rpt4 ssd1-d* strains, however, as they are not prevented by osmotic stabilization (data not shown). Although the *rpt4-145 SSD1* strain displays no defects in SPB duplication, the *rpt4-150 SSD1* strain exhibits a monopolar arrest at restrictive temperature.

The as-yet-undefined role of Rpt4p in SPB duplication appears to be required early in this process. Analysis of other conditional mutations that specifically affect SPB duplication have previously revealed several distinct patterns of failure. For example, *mps2* (Winey *et al.* 1991), *ndc1* (Winey *et al.* 1993), and *bbp1* (Schramm *et al.* 2000) mutants display failure relatively late, such that a duplication plaque is assembled on the half-bridge, but is not inserted into the nuclear envelope. In contrast, *cdc31* (Byers 1981b), *kar1* (Rose and Fink 1987), *mps1-1* (Winey *et al.* 1991), *dsk2*Δ *rad23*Δ (Biggins *et al.* 1996), and *rpt4* mutants fail earlier, such that the satellite, the earliest visible precursor to the nascent SPB, does not form or is not maintained. Interestingly, multiple genetic interactions have been observed between several members of this latter group of SPB duplication genes (*DSK2*, *RAD23*, *KAR1*, *CDC31*) and the protein kinase C pathway, suggesting that this pathway is involved in SPB duplication (Khalfan *et al.* 2000). This finding might ultimately provide insight into the *rpt4* SPB duplication defects, given that *SSD1* interacts genetically with *RPT4* and the protein kinase C pathway.

An additional later role for Rpt4p in SPB assembly or maintenance is suggested by the presence of imbalanced spindles in *rpt4-145 ssd1-d* and *rpt4-150 ssd1-d* strains. These spindles are organized by SPBs that can vary quite dramatically in size and appear to organize different numbers of microtubules (Figure 6), suggesting that the smaller SPB was not fully formed or maintained at restrictive temperature. Mutations in *SPC29*, which encodes a component of the SPB and the satellite (Wigge *et al.* 1998; Adams and Kilmartin 1999), can also result in SPB duplication defects (Elliott *et al.* 1999) or complete/broken spindles containing SPBs of unequal size (Adams and Kilmartin 1999).

SPB duplication in yeast serves as a model for under-

standing centrosome duplication in higher eukaryotic cells (Adams and Kilmartin 2000). Although morphologically dissimilar, the SPB and centrosome share some common components, and the regulatory mechanisms governing centrosome and SPB duplication show similarity as well. For example, a mouse ortholog of Mps1p has been shown to regulate centrosome duplication in cultured mouse cells (Fisk and Winey 2001). Links between the proteasome degradation system and centrosome duplication have also been established. For example, proteasomal components (Wigley *et al.* 1999) and ubiquitin ligase components (Freed *et al.* 1999; Gstaiger *et al.* 1999) are associated with the centrosome and regulate its duplication cycle in Xenopus (Freed *et al.* 1999). Mutations in ubiquitin ligase components result in centrosome overduplication in mouse (Nakayama *et al.* 2000) and Drosophila cells (Wojcik *et al.* 2000). In the former case, this defect appears to arise at least partially from a lack of cyclin E degradation. In light of these results, it will be interesting to determine whether the mammalian Rpt4 subunit, p42 (Fujiwara *et al.* 1996), in which the residues corresponding to those affected by the *rpt4-145* and *rpt4-150* mutations are largely conserved, has a specific role in centrosome duplication or assembly.

We thank Dr. Breck Byers for support and useful discussion, Dr. Robert Coyne for useful comments on the manuscript, Dr. James Haber for providing the *crl13* strain, and Melanie Randall for participating in early phases of this project. The work at Colgate University was supported by a National Science Foundation grant (MCB-9727240) to H. B. McDonald. L. Goetsch's work was supported by National Institutes of Health grant GM-18541 to Dr. Breck Byers.

LITERATURE CITED

Adams, I. R., and J. V. Kilmartin, 1999 Localization of core spindle pole body (SPB) components during SPB duplication in *Saccharomyces cerevisiae*. J. Cell Biol. **145:** 809–823.

Adams, I. R., and J. V. Kilmartin, 2000 Spindle pole body duplication: A model for centrosome duplication? Trends Cell Biol. **10:** 329–335.

Altschul, S. F., W. Gish, W. Miller, E. W. Myers and D. J. Lipman, 1990 Basic local alignment search tool. J. Mol. Biol. **215:** 403–410.

Ausubel, F. M., R. Brent, R. E. Kingston, D. D. Moore, J. G. Seidman *et al.* (Editors), 1994 *Current Protocols in Molecular Biology*. John Wiley & Sons, New York.

Bass, S. H., M. G. Mulkerrin and J. A. Wells, 1991 A systematic mutational analysis of hormone-binding determinants in the human growth hormone receptor. Proc. Natl. Acad. Sci. USA **88:** 4498–4502.

Baudin, A., O. Ozier-Kalogeropoulos, A. Denouel, F. Lacroute and C. Cullin, 1993 A simple and efficient method for direct gene deletion in *Saccharomyces cerevisiae*. Nucleic Acids Res. **21:** 3329–3330.

Bennett, W. F., N. F. Paoni, B. A. Keyt, D. Botstein, A. J. S. Jones *et al.*, 1991 High resolution analysis of functional determinants on human tissue-type plasminogen activator. J. Biol. Chem. **266:** 5191–5201.

Beyer, A., 1997 Sequence analysis of the AAA protein family. Protein Sci. **6:** 2043–2058.

Biggins, S., I. Ivanovska and M. D. Rose, 1996 Yeast ubiquitin-like genes are involved in duplication of the microtubule organizing center. J. Cell Biol. **133:** 1331–1346.

Boeke, J. D., F. LaCroute and G. R. Fink, 1984 A positive selection for mutants lacking orotidine-5′-phosphate decarboxylase activity in yeast: 5-fluoro-orotic acid resistance. Mol. Gen. Genet. **197:** 345–346.

Brachmann, C. B., A. Davies, G. J. Cost, E. Caputo, J. Li *et al.*, 1998 Designer deletion strains derived from *Saccharomyces cerevisiae* S288C: a useful set of strains and plasmids for PCR-mediated gene disruption and other applications. Yeast **14:** 115–132.

Braun, B. C., M. Glickman, R. Kraft, B. Dahlmann, P.-M. Kloetzel *et al.*, 1999 The base of the proteasome regulatory particle exhibits chaperone-like activity. Nat. Cell Biol. **1:** 221–226.

Byers, B., 1981a Cytology of the yeast life cycle, pp. 59–96 in *Molecular Biology of the Yeast Saccharomyces*, edited by J. N. Strathern, E. W. Jones and J. R. Broach. Cold Spring Harbor Laboratory Press, Cold Spring Harbor, NY.

Byers, B., 1981b Multiple roles of the spindle pole bodies in the life cycle of *Saccharomyces cerevisiae*, pp. 119–133 in *Molecular Genetics in Yeast: Alfred Benzon Symposia 16*, edited by D. von Wettstein, J. Friis, M. Kielland-Brandt and A. Stenderup. Munksgaard, Copenhagen.

Byers, B., and L. Goetsch, 1991 Preparation of yeast cells for thin-section electron microscopy, pp. 602–607 in *Methods in Enzymology*, edited by C. Guthrie and G. R. Fink. Academic Press, San Diego.

Ciechanover, A., 1998 The ubiquitin-proteasome pathway: on protein death and cell life. EMBO J. **17:** 7151–7160.

Cunningham, B. C., and J. A. Wells, 1989 High-resolution epitope mapping of hGF-receptor interactions by alanine-scanning mutagenesis. Science **244:** 1081–1085.

Cvrcková, F., and K. Nasmyth, 1993 Yeast G1 cyclins CLN1 and CLN2 and a GAP-like protein have a role in bud formation. EMBO J. **12:** 5277–5286.

Dohmen, R. J., P. Wu and A. Varshavsky, 1994 Heat-inducible degron: a method for constructing temperature-sensitive mutants. Science **263:** 1273–1276.

Doseff, A. I., and K. T. Arndt, 1995 LAS1 is an essential nuclear protein involved in cell morphogenesis and cell surface growth. Genetics **141:** 857–871.

Elliott, S., M. Knop, G. Schlenstedt and E. Schiebel, 1999 Spc29p is a component of the Spc110p subcomplex and is essential for spindle pole body duplication. Proc. Natl. Acad. Sci. USA **96:** 6205–6210.

Enenkel, C., A. Lehmann and P.-M. Kloetzel, 1998 Subcellular distribution of proteasomes implicates a major location of protein degradation in the nuclear envelope-ER network in yeast. EMBO J. **17:** 6144–6154.

Ferdous, A., F. Gonzalez, L. Sun, T. Kodadek and S. A. Johnston, 2001 The 19S regulatory particle of the proteasome is required for efficient transcription elongation by RNA polymerase II. Mol. Cell **7:** 981–991.

Ferrell, K., C. R. M. Wilkinson, W. Dubiel and C. Gordon, 2000 Regulatory subunit interactions of the 26S proteasome: a complex problem. Trends Biochem. Sci. **25:** 83–88.

Finley, D., K. Tanaka, C. Mann, H. Feldmann, M. Hochstrasser *et al.*, 1998 Unified nomenclature for subunits of the *Saccharomyces cerevisiae* proteasome regulatory particle. Trends Biochem. Sci. **23:** 244–245.

Fisk, H. A., and M. Winey, 2001 The mouse Mps1p-like kinase regulates centrosome duplication. Cell **106:** 95–104.

Flemington, E., and S. H. Speck, 1990 Evidence for coiled-coil dimer formation by an Epstein-Barr virus transactivator that lacks a heptad repeat of leucine residues. Proc. Natl. Acad. Sci. USA **87:** 9459–9463.

Freed, E., K. R. Lacey, P. Huie, S. A. Lyapina, R. J. Deshaies *et al.*, 1999 Components of an SCF ubiquitin ligase localize to the centrosome and regulate the centrosome duplication cycle. Genes Dev. **13:** 2242–2257.

Fujiwara, T., T. K. Watanabe, K. Tanaka, C. A. Slaughter and G. N. DeMartino, 1996 cDNA cloning of p42, a shared subunit of two proteasome regulatory proteins, reveals a novel member of the AAA protein family. FEBS Lett. **387:** 184–188.

Ghislain, M., A. Udvardy and C. Mann, 1993 *S. cerevisiae* 26S protease mutants arrest cell division in G2/metaphase. Nature **366:** 358–362.

Gietz, D., A. St. Jean, R. A. Woods and R. H. Schiestl, 1992 Improved method for high efficiency transformation of intact yeast cells. Nucleic Acids Res. **20:** 1425.

Gillette, T. G., W. Huang, S. J. Russell, S. H. Reed, S. A. Johnston *et al.*, 2001 The 19S complex of the proteasome regulates nucleotide excision repair in yeast. Genes Dev. **15:** 1528–1539.

Glickman, M. H., D. M. Rubin, O. Coux, I. Wefes, G. Pfeifer *et al.*, 1998a A subcomplex of the proteasome regulatory particle required for ubiquitin-conjugate degradation and related to the COP9-signalosome and eIF3. Cell **94:** 615–623.

Glickman, M. H., D. M. Rubin, V. A. Fried and D. Finley, 1998b The regulatory particle of the *Saccharomyces cerevisiae* proteasome. Mol. Cell. Biol. **18:** 3149–3162.

Gonzalez, F., A. Delahodde, T. Kodadek and S. A. Johnston, 2002 Recruitment of a 19S proteasome subcomplex to an activated promoter. Science **296:** 548–550.

Groll, M., L. Ditzel, J. Löwe, D. Stock, M. Bochtler *et al.*, 1997 Structure of 20S proteasome from yeast at 2.4 Å resolution. Nature **386:** 463–471.

Groll, M., M. Bajorek, A. Köhler, L. Moroder, D. M. Rubin *et al.*, 2000 A gated channel into the proteasome core particle. Nat. Struct. Biol. **7:** 1062–1067.

Gstaiger, M., A. Marti and W. Krek, 1999 Association of human SCF (SKP2) subunit p19 (SKP1) with interphase centrosomes and mitotic spindle poles. Exp. Cell Res. **247:** 554–562.

Hartwell, L. H., 1967 Macromolecule synthesis in temperature-sensitive mutants of yeast. J. Bacteriol. **93:** 1662–1670.

Heinisch, J. J., A. Lorberg, H. P. Schmitz and J. J. Jacoby, 1999 The protein kinase C-mediated MAP kinase pathway involved in the maintenance of cellular integrity in *Saccharomyces cerevisiae*. Mol. Microbiol. **32:** 671–680.

Hershko, A., and A. Ciechanover, 1998 The ubiquitin system. Annu. Rev. Biochem. **67:** 425–479.

Hu, J. C., E. K. O'Shea, P. S. Kim and R. T. Sauer, 1990 Sequence requirements for coiled-coils: analysis with lambda repressor-GCN4 leucine zipper fusions. Science **250:** 1400–1403.

Hutter, K. J., and H. E. Eipel, 1979 Microbial determination by flow cytometry. J. Gen. Microbiol. **113:** 369–375.

Jacobs, C. W., A. E. M. Adams, P. J. Szaniszlo and J. R. Pringle, 1988 Functions of microtubules in the *Saccharomyces cerevisiae* cell cycle. J. Cell Biol. **107:** 1409–1426.

Kaeberlein, M., and L. Guarente, 2002 *Saccharomyces cerevisiae MPT5* and *SSD1* function in parallel pathways to promote cell wall integrity. Genetics **160:** 83–95.

Khalfan, W., I. Ivanovska and M. D. Rose, 2000 Functional interaction between the *PKC1* pathway and *CDC31* network of SPB duplication genes. Genetics **155:** 1543–1559.

Kilmartin, J. V., and A. E. M. Adams, 1984 Structural rearrangements of tubulin and actin during the cell cycle of the yeast *Saccharomyces*. J. Cell Biol. **98:** 922–933.

King, R. W., R. J. Deshaies, J.-M. Peters and M. W. Kirschner, 1996 How proteolysis drives the cell cycle. Science **274:** 1652–1659.

Koepp, D. M., J. W. Harper and S. J. Elledge, 1999 How the cyclin became a cyclin: regulated proteolysis in the cell cycle. Cell **97:** 431–434.

Köhler, A., P. Cascio, D. S. Leggett, K. M. Woo, A. L. Goldberg *et al.*, 2001 The axial channel of the proteasome core particle is gated by the Rpt2 ATPase and controls both substrate entry and product release. Mol. Cell **7:** 1143–1152.

Kunau, W. H., A. Beyer, T. Franken, K. Gotte, M. Marzioch *et al.*, 1993 Two complementary approaches to study peroxisome biogenesis in *Saccharomyces cerevisiae*: forward and reversed genetics. Biochimie **75:** 209–224.

Laemmli, U. K., 1970 Cleavage of structural proteins during the assembly of the head of bacteriophage T4. Nature **227:** 680–685.

Lupas, A., M. Van Dyke and J. Stock, 1991 Predicting coiled coils from protein sequences. Science **252:** 1162–1164.

McCusker, J. H., and J. E. Haber, 1988 Cycloheximide-resistant temperature-sensitive lethal mutations of *Saccharomyces cerevisiae*. Genetics **119:** 303–315.

McDonald, H., and B. Byers, 1997 A proteasome cap subunit required for spindle pole body duplication in yeast. J. Cell Biol. **137:** 539–553.

Mortimer, R., and D. Hawthorne, 1969 Yeast genetics, pp. 385–460 in *The Yeasts*, edited by A. H. Rose and J. S. Harrison. Academic Press, New York.

Nakayama, K., H. Nagahama, Y. A. Minamishima, M. Matsumoto, I. Nakamichi *et al.*, 2000 Targeted disruption of *Skp2* results in accumulation of cyclin E and $p27^{Kip1}$, polyploidy and centrosome overduplication. EMBO J. **19:** 2069–2081.

Pellegrino, S., S. Zhang, A. Garritsen and W. F. Simonds, 1997 The coiled-coil region of the G protein β subunit. J. Biol. Chem. **272:** 25360–25366.

Rechsteiner, M., L. Hoffman and W. Dubiel, 1993 The multicatalytic and 26 S proteases. J. Biol. Chem. **268:** 6065–6068.

Reijo, R. A., E. M. Cooper, G. J. Beagle and T. C. Huffaker, 1994 Systematic mutational analysis of the yeast β-tubulin gene. Mol. Biol. Cell **5:** 29–43.

Reits, E. A. J., A. M. Benham, B. Plougastel, J. Neefjes and J. Trowsdale, 1997 Dynamics of proteasome distribution in living cells. EMBO J. **16:** 6087–6094.

Richmond, C., C. Gorbea and M. Rechsteiner, 1997 Specific interactions between ATPase subunits of the 26 S protease. J. Biol. Chem. **272:** 13403–13411.

Robbins, J., S. M. Dilworth, R. A. Laskey and C. Dingwall, 1991 Two interdependent basic domains in nucleoplasmin nuclear targeting sequence: identification of a class of bipartite nuclear targeting sequence. Cell **64:** 615–623.

Rose, M. D., and G. R. Fink, 1987 *KAR1*, a gene required for function of both intranuclear and extranuclear microtubules in yeast. Cell **48:** 1047–1060.

Rubin, D. M., M. H. Glickman, C. N. Larsen, S. Dhruvakumar and D. Finley, 1998 Active site mutants in the six regulatory particle ATPases reveal multiple roles for ATP in the proteasome. EMBO J. **17:** 4909–4919.

Russell, S. J., S. H. Reed, W. Huang, E. C. Friedberg and S. A. Johnston, 1999a The 19S regulatory complex of the proteasome functions independently of proteolysis in nucleotide excision repair. Mol. Cell **3:** 687–695.

Russell, S. J., K. A. Steger and S. A. Johnston, 1999b Subcellular localization, stoichiometry, and protein levels of 26S proteasome subunits in yeast. J. Biol. Chem. **274:** 21943–21952.

Russell, S. J., F. Gonzalez, L. Joshua-Tor and S. A. Johnston, 2001 Selective chemical inactivation of AAA proteins reveals distinct functions of proteasomal ATPases. Chem. Biol. **8:** 941–950.

Sambrook, J., E. F. Fritsch and T. Maniatis, 1989 *Molecular Cloning: A Laboratory Manual*. Cold Spring Harbor Laboratory Press, Cold Spring Harbor, NY.

Schramm, C., S. Elliott, A. Shevchenko and E. Schiebel, 2000 The Bbp1p-Mps2p complex connects the SPB to the nuclear envelope and is essential for SPB duplication. EMBO J. **19:** 421–433.

Sikorski, R. S., and P. Hieter, 1989 A system of shuttle vectors and yeast host strains designed for efficient manipulation of DNA in *Saccharomyces cerevisiae*. Genetics **122:** 19–27.

Sutton, A., D. Immanuel and K. T. Arndt, 1991 The SIT4 protein phosphatase functions in late G1 for progression into S phase. Mol. Cell. Biol. **11:** 2133–2148.

Takeuchi, J., and A. Toh-e, 1999 Genetic evidence for interaction between components of the yeast 26S proteasome: combination of a mutation in *RPN12* (a lid component gene) with mutations in *RPT1* (an ATPase gene) causes synthetic lethality. Mol. Gen. Genet. **262:** 145–153.

Tyers, M., and P. Jorgensen, 2000 Proteolysis and the cell cycle: with this RING I do thee destroy. Curr. Opin. Genet. Dev. **10:** 54–64.

Uesono, Y., A. Toh-e and Y. Kikuchi, 1997 Ssd1p of *Saccharomyces cerevisiae* associates with RNA. J. Biol. Chem. **272:** 16103–16109.

Voges, D., P. Zwickl and W. Baumeister, 1999 The 26S proteasome: a molecular machine designed for controlled proteolysis. Annu. Rev. Biochem. **68:** 1015–1068.

Walker, J. E., M. Saraste, M. J. Runswick and N. J. Gay, 1982 Distantly related sequences in the alpha- and beta-subunits of ATP synthase, myosin, kinases and other ATP-requiring enzymes and a common nucleotide binding fold. EMBO J. **1:** 945–951.

Wang, W., P. M. Chevray and D. Nathans, 1996 Mammalian Sug1 and c-Fos in the nuclear 26S proteasome. Proc. Natl. Acad. Sci. USA **93:** 8236–8240.

Wertman, K. F., D. G. Drubin and D. Botstein, 1992 Systematic mutational analysis of the yeast *ACT1* gene. Genetics **132:** 337–350.

Wigge, P. A., O. N. Jensen, S. Holmes, S. Souès, M. Mann *et al.*, 1998 Analysis of the *Saccharomyces* spindle pole by matrix-assisted

laser desorption/ionization (MALDI) mass spectrometry. J. Cell Biol. **141:** 967–977.

Wigley, W. C., R. P. Fabunmi, M. G. Lee, C. R. Marino, S. Muallem *et al.*, 1999 Dynamic association of proteasomal machinery with the centrosome. J. Cell Biol. **145:** 481–490.

Wilkinson, C. R. M., M. Wallace, M. Morphew, P. Perry, R. Allshire *et al.*, 1998 Localization of the 26S proteasome during mitosis and meiosis in fission yeast. EMBO J. **17:** 6465–6476.

Winey, M., L. Goetsch, P. Baum and B. Byers, 1991 *MPS1* and *MPS2*: novel yeast genes defining distinct steps of spindle pole body duplication. J. Cell Biol. **114:** 745–754.

Winey, M., M. A. Hoyt, C. Chan, L. Goetsch, D. Botstein *et al.*, 1993 *NDC1*: a nuclear periphery component required for yeast spindle pole body duplication. J. Cell Biol. **122:** 743–751.

Wojcik, E. J., D. M. Glover and T. S. Hays, 2000 The SCF ubiquitin ligase protein Slimb regulates centrosome duplication in *Drosophila*. Curr. Biol. **10:** 1131–1134.

Zwickl, P., W. Baumeister and A. Steven, 2000 Dis-assembly lines: the proteasome and related ATPase-assisted proteases. Curr. Opin. Struct. Biol. **10:** 242–250.

Communicating editor: M. Johnston